ELSEVIER

Cement & Concrete Composites 26 (2004) 359–370

Cement & Concrete Composites

www.elsevier.com/locate/cemconcomp

Acoustic performance and damping behavior of cellulose–cement composites

Narayanan Neithalath, Jason Weiss *, Jan Olek

School of Civil Engineering, Purdue University, 1284 Civil Engineering Building, West Lafayette, IN 47907-1284, USA

Received 10 September 2002; accepted 23 December 2002

Abstract

This paper describes the influence of morphologically altered cellulose fibers on the acoustic and mechanical properties of cellulose–cement composites. Three fiber morphologies were considered (macro-nodules, discrete fibers, and petite nodules). The main parameters studied include the normal incident acoustic absorption coefficient (α), specific damping capacity (ψ), loss tangent ($\tan\delta$), storage modulus (E'), and loss modulus ($E'' = E'\tan\delta$). The acoustic absorption coefficient was found to increase with an increase in fiber volume for all three fiber types investigated, though "macro-nodule" fibers were found to be the most effective. Stiffness–loss relationships are reported for these composites and the behavior of cellulose–cement composites with soft cellulose fiber inclusions was found to be similar to a Voigt (series) composite model. Low volumes of fibers had a minimal effect on the loss tangent; however the stiffness was considerably reduced. Predictive equations for loss modulus as a function of fiber volume at different moisture conditions were developed. These relations compare well with the experimental values as well as the idealized Voigt composite behavior. This suggests that there is an optimum fiber volume, which maximizes the loss modulus for saturated composites while the loss modulus is practically independent of fiber volume for dry composites.

Keywords: Acoustic absorption; Cellulose–cement composite; Fiber morphology; Loss modulus; Rule of mixtures; Specific damping capacity

1. Introduction

Fibers are used in cementitious matrices primarily to modify the tensile and flexural strengths, toughness, impact resistance, and fracture energy [1]. Cellulose–cement composites are mainly used for two reasons: (i) they are light at high volumes of fibers, and (ii) they can be manufactured with cost–performance ratios comparable to other building materials [2]. Wood–cement composites generally fall into two categories: wood particle–cement composites and wood fiber reinforced cement composites. Wood particle composites are primarily of architectural value whereas wood fiber reinforced composites can be used as structural materials [3]. Several studies have examined the effectiveness of both virgin and recycled cellulose fibers as well wood chippings and shavings in cementitious systems [4,5]. Cellulose fiber–cement composites have found applications in production of thin and flat corrugated cement sheets, noise barriers for highways, and residential wallboards. Several studies have reported the influence of cellulose fibers on the fresh and hardened properties of cementitious materials [5–9]. The use of fiber reinforcement has been reported to increase the flexural strength in dry condition and decrease it in wet condition [2], while the compressive strength is frequently reported to decrease with increase in fiber content [3,10,11].

Though it has been mentioned by some researchers that natural fiber–cement composites can be used for noise control purposes [10], only limited data exists on their acoustic characteristics. As far as acoustic studies on fibers and flakes are concerned, Wassilieff [12] has elaborated on sound absorption of compressed wood fibers and flakes by considering them as agglomeration of slit shaped channels, which allow sound waves to pass through.

As is evident from the foregoing discussion on previous research using cellulose–cement composites, there has been considerable study on the physical and mechanical properties of this material, which has

* Corresponding author. Tel.: +1-765-494-2215; fax: +1-765-496-1364.

E-mail address: wjweiss@ecn.purdue.edu (J. Weiss).

0958-9465/$ - see front matter © 2003 Elsevier Ltd. All rights reserved.
doi:10.1016/S0958-9465(03)00020-9

been looked upon mainly as a material with higher toughness. While the shape and volume fraction of different fibers are frequently investigated with respect to their impact on fresh composite properties and mechanical behavior [1,13,14], this paper explores the option of using morphologically altered cellulose fibers to develop cementitious composites with enhanced acoustic and damping characteristics.

2. Research significance

The research work presented in this paper has been initiated on the premise that the pore network of cement-based materials can be tailored to absorb sound and dissipate structure-borne vibrations. The purpose of this paper is to discuss the influence of the volume and morphology of cellulose fibers on the sound absorption and vibration damping characteristics of cellulose–cement composites. Specifically, this paper compares the acoustic effectiveness and damping features of morphologically altered cellulose fiber–cement composites. The results presented in this paper would be of interest to engineers involved in designing quieter wall panels, structural components and pavements.

3. Experimental program

3.1. Materials and mixture proportions

3.1.1. Fiber types

The three types of cellulose fibers used in this study are shown in Fig. 1. The first type consisted of fiber agglomerates (nodules), ranging from 1 to 8 mm in size, formed by a flaking process that did not separate the fibers during manufacture. For the scope of this paper, they will be termed *macro-nodules*. The second type consisted of typical cellulose fibers, 2–3 mm long and 20–60 μm in diameter and is referred to as *discrete fibers*. The third type consisted of a mixture of small fiber nodules and normal short fibers, and will be referred to as *petite nodules*. All the fibers were bleached soft wood fibers. The latter two types of fibers, discrete fibers and petite nodules, to a certain degree, could be dispersed fairly easily into individual units in water whereas macro-nodules were not easily dispersible. The fiber

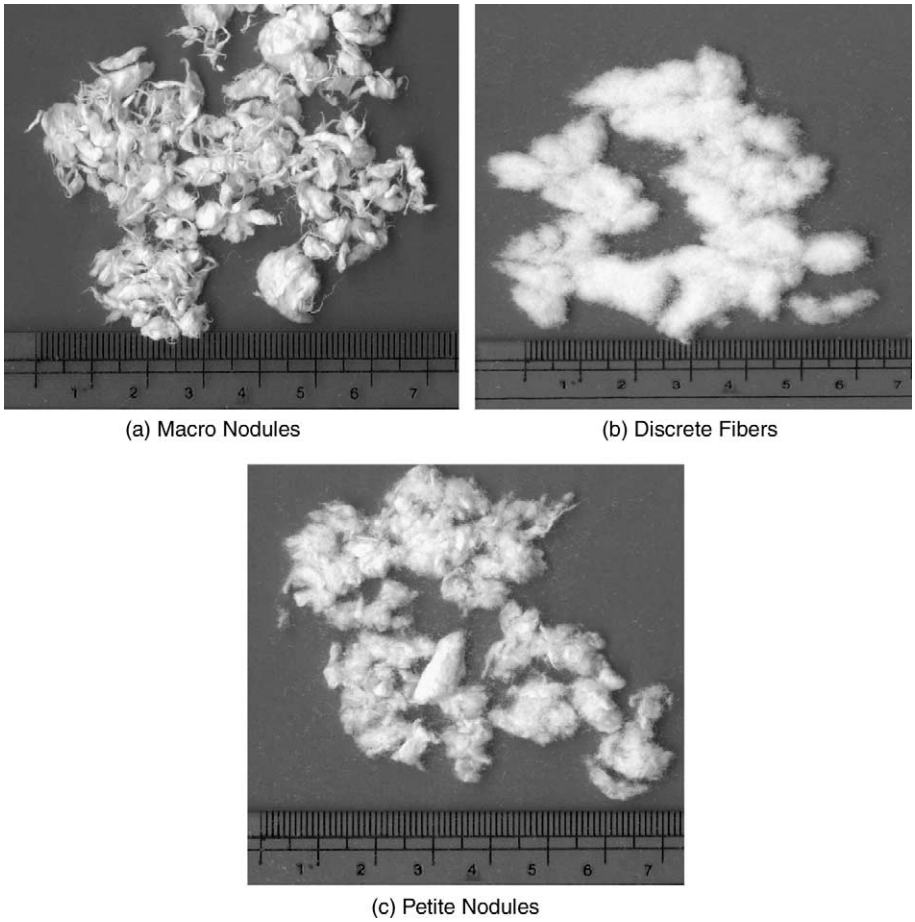

Fig. 1. Morphology of three types of cellulose fibers used in this study (scale shown in cm).

nodules or clumps are porous since they are formed by the agglomeration of individual fibers.

3.1.2. Composition of mortar mixtures

A cement–sand mortar, with 50% of sand by volume of the matrix phase has been used throughout this study. The cement used was an ASTM Type I. Fiber volume chosen for the three selected fibers varied with the type of fiber. For macro-nodule fibers, 1.5%, 3.0%, 4.5%, 6.0% and 7.5% of the matrix volume was replaced by fibers whereas for discrete fibers and petite nodules, 1.5%, 3.0% and 4.5% replacement was chosen. Two different series of fiber volumes were selected based on two criteria: (i) macro-nodules, by virtue of their particle size and porosity, were assumed to provide the kind of porosity that could be beneficial for sound absorption and (ii) at higher volumes, discrete fibers and petite nodules tend to clump together in the matrix and the water content required to achieve desired consistency increases drastically. In contrast, macro-nodules being more "aggregate-like" retain their physical form during mixing and require less water to reach the desired consistency.

For all fibers, the water demand increased with the addition of fibers to the mixture. Since the addition of water reducer was not effective in maintaining constant water–cement ratio (w/c) for all mixtures, the w/c was adjusted to maintain fresh mix workability at a reasonably practical level, represented by flow values determined in accordance with ASTM C 1437 [15]. Table 1 gives the details of the fresh properties of the mixtures.

3.2. Mixing procedures

The mixing procedure adopted in this study was varied depending on the type of fibers that were used. For mixtures with macro-nodules, cement and sand was first mixed at low speed for 1 min and then the fibers were added, while mixing. Approximately three quarters of the water needed was added and all ingredients were mixed at medium speed for 2 min. The remaining water was then added with water reducer and mixed until a uniform mixture was obtained (typically at 1 min). Care was taken to ensure that the mixer did not run at higher than required speeds or for longer than required durations so that the fiber nodules are not broken down in the mixer. For mixtures with high volumes of fiber (6.0% and 7.5%), an accelerator was added since it was noticed that there was considerable set retardation otherwise. Discrete fibers and petite nodules were initially mixed with about three quarters of the mixing water for 1 min while the mixer was running at low speed. This enabled the fibers to be dispersed. Cement and sand were then added and mixed at medium speed for 2 min, stopped for 1 min, followed by the addition of remaining water and water reducer till a uniform mixture was obtained.

For each mixture, cylindrical specimens were cast for acoustic absorption (95 mm diameter, 100 mm long) and compressive strength (75 mm diameter, 150 mm long), and prismatic specimens for specific damping capacity and flexural strength (250 mm $\times$ 75 mm $\times$ 25 mm) determination. All the specimens were consolidated using external vibration and were kept damp inside the molds for 24 h, after which they were moist cured (at >98% RH, 23 °C) until the test age. Slices (75 mm $\times$ 25 mm $\times$ 25mm) were cut from the prismatic specimens for porosity determination.

3.3. Experimental methods

3.3.1. Porosity determination

Porosity was determined on 75 mm $\times$ 75 mm $\times$ 25 mm prisms of composite specimens obtained as mentioned in the previous section. The method of vacuum saturation as described in RILEM CPC 11.3 [16] has been followed in the determination of porosity. The prisms were dried in an oven at 105 ± 5 °C until no change in measured weight was noticed. The specimens

Table 1
Ingredients and flow characteristics of the mixtures

Fiber type	Fiber volume (%)	Water–cement ratio	Water reducer (% by weight of cement)	Accelerator (% by weight of cement)	Flow ±5 (%)
–	0.0	0.47	0.0	0	70
Macro-nodules	1.5	0.50	1.0	0	65
	3.0	0.52	1.0	0	55
	4.5	0.57	1.5	0	55
	6.0	0.65	2.0	1	50
	7.5	0.69	2.5	1	45
Discrete fibers	1.5	0.50	1.0	0	70
	3.0	0.52	1.0	0	65
	4.5	0.56	1.5	0	55
Petite nodules	1.5	0.50	1.0	0	70
	3.0	0.52	1.0	0	60
	4.5	0.57	1.5	0	55

were then kept dry in a vacuum chamber for 3 h before water was introduced to the chamber, under vacuum. The vacuum was maintained for 6 more hours after which time the specimens were left in water for 18 h. The saturated surface dried weight was then determined. For the fiber-reinforced specimens, the water absorbed by the fibers was accounted for in the vacuum saturated weight so as to obtain the effective porosity. Porosity of a plain (control) mortar was also determined. These porosities were used to calculate the normalized porosity as reported in Section 4.1.1.

3.3.2. Measurement of absorption coefficient by impedance tube

To evaluate the acoustical characteristics of cellulose–cement composites, the normal incident absorption coefficient (α) was determined for different fiber volumes for all three types of fibers. The absorption coefficient is a measure of how well a material can absorb sound. When a sound wave strikes a material, a portion of the sound energy is reflected back while a portion is absorbed by the material. The absorption coefficient is the ratio of the absorbed energy to the total incident energy.

The impedance tube was used to determine the absorption coefficient using the experimental set up shown in Fig. 2. The measurement is based on the two-microphone transfer function test method, making simultaneous measurements at all frequencies of interest, as described in ASTM E-1050 [17]. The sample is placed at one end of the cylindrical tube with a rigid backing. The specimen is tested with a plane acoustic wave propagating along the axis of the tube. The absorption coefficient is calculated as

$$\alpha = 1 - |R|^2 \tag{1}$$

where the reflection coefficient (R) is computed for frequencies ranging from 100 to 1600 Hz using the following equation:

$$R = \frac{e^{jkd_1} - e^{jkd_2}P}{e^{-jkd_2}P - e^{-jkd_1}} \tag{2}$$

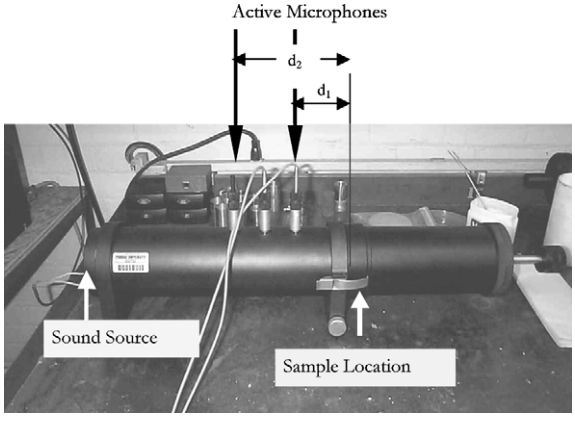

Fig. 2. Impedance tube set up for determining absorption coefficient.

d_1 and d_2 are the distances from the specimen surface to the first and second microphones respectively (Fig. 2), j is $\sqrt{-1}$, k is the wave number (ratio of angular frequency to the wave speed in the medium), and P is the ratio of acoustic pressures.

3.3.3. Dynamic elastic modulus

The dynamic modulus of elasticity of composite specimens was calculated from the resonant frequency following the procedure described in ASTM C 1259-01 [18], using Grindosonic™ equipment. The specimens were supported at their flexural nodal points (0.224L from supports) and excited to obtain the fundamental flexural resonant frequency.

3.3.4. Specific damping capacity

The specific damping capacity (ψ) was determined using Grindosonic™ equipment according to the decaying sin wave method.

$$\psi = \frac{A_i - A_{n+i}}{A_i} \times 100\% \tag{3}$$

where A_i is the amplitude of the ith period and A_{n+i}, that of $(n+i)$th period.

4. Analysis and discussion of the results

4.1. Porosity

For sound absorbing materials, porosity (ϕ) is one of the primary factors that govern its acoustic behavior. The attenuation of sound is believed to be effected by the porosity incorporated into the system by the addition of porous fiber nodules or clumps. Porosity also plays a significant role in determining the mechanical properties of the composite.

4.1.1. Influence of fiber volume and morphology on porosity

A plot of normalized porosity ($\phi_{composite}/\phi_{mortar}$) versus fiber volume for composites with all the three fiber types is shown in Fig. 3. It can be observed from this figure that the increase in porosity is highest for specimens with macro-nodules and lowest for those with discrete fibers. The relationship is linear (R^2 values of 0.93, 0.99 and 0.87 for macro-nodules, petite nodules and discrete fibers respectively), with porosity increasing with fiber volume. The relationship between the porosity of the composite at any fiber volume and the porosity of the mortar can be given by

$$\phi_{composite} = \phi_{mortar}(1 + A\ V_f) \tag{4}$$

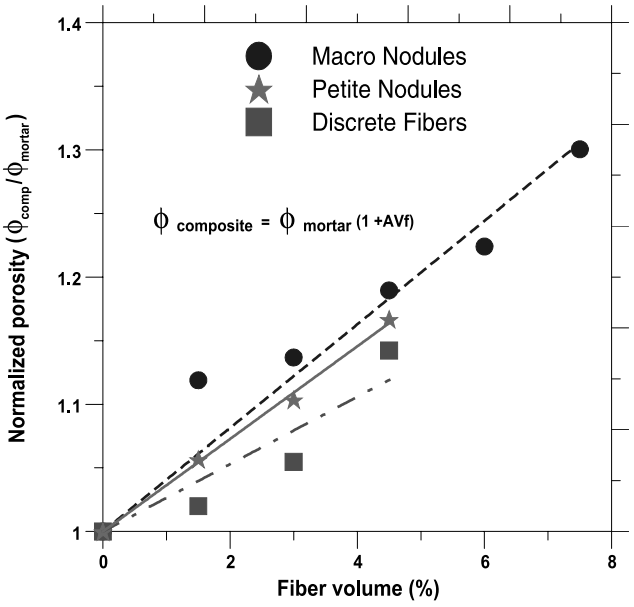

Fig. 3. Influence of fiber volume and morphology on composite porosity.

where the value of the constant A can be considered as an indicator of the contribution of the fiber phase to the total porosity of the composite. In the present study, the constant A assumes values of 0.041, 0.036 and 0.023 for composites with macro-nodules, petite nodules and discrete fibers respectively.

The increase in porosity with increasing fiber volume in mixtures containing macro-nodules and petite nodules can be explained by the fact that in addition to being porous themselves, these nodules are composed of porous fibers that can absorb water. For specimens with discrete fibers, the increased porosity may be due to the tendency of fibers to clump together while mixing, entrapping water-filled spaces, which consequently turn into voids. Increased fiber volume enhances the potential for fiber clumping.

4.2. Acoustic absorption coefficient

4.2.1. Influence of fiber volume and morphology on absorption coefficient

Cylindrical specimens (95 mm diameter and 75 mm long, cut from 100 mm long specimens) were tested in an air dry state to obtain the absorption spectra (plot of absorption coefficients at different frequencies) for composites with varying volumes of fiber. The spectra for composites with macro-nodules as inclusions are given in Fig. 4(a). For the 75 mm long specimens, the absorption peak occurs at a frequency of approximately 500 Hz. It can be seen that an increase in fiber content increases the maximum absorption coefficient. For a sample with no fiber, maximum α is approximately 0.05 and it steadily increases to approximately 0.40 for the composite with 7.5% volume of macro-nodules. The macro-nodules appear to provide porous channels inside the specimen where the incident sound energy can enter and attenuate. With an increase in fiber volume, it is expected that there is an increase in the number of connected porous channels, leading to an increase in sound absorption. Discrete fibers and petite nodules are less effective in acoustic absorption, showing only about 50% of the improvement shown by the composites with macro-nodules (Fig. 4(b)). This observation justifies the premise that fiber morphology has a significant influence on the acoustic absorption behavior of the composite.

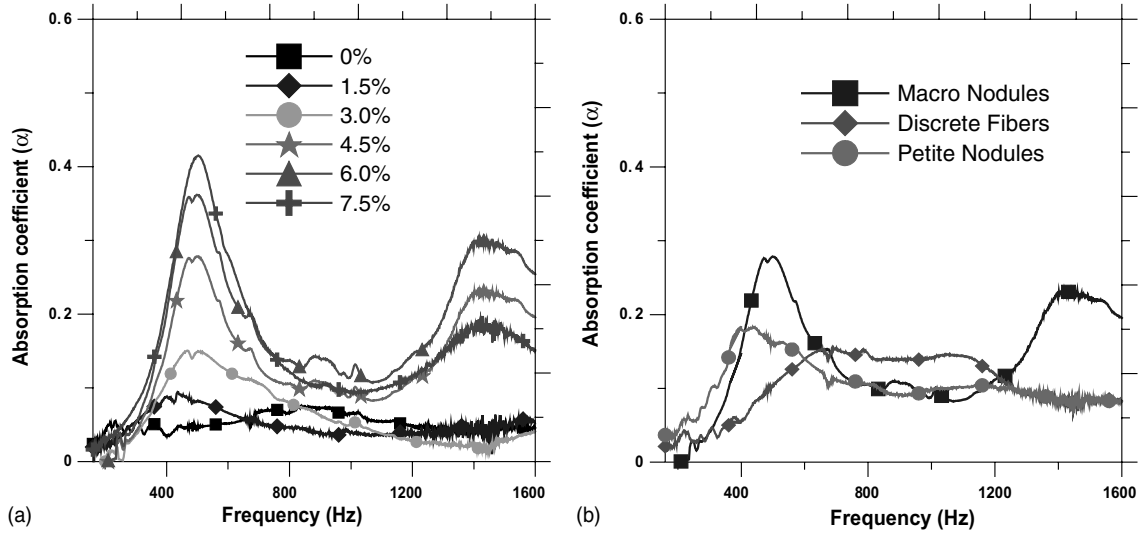

Fig. 4. (a) Acoustic absorption spectra of composites with macro-nodules; (b) comparison of absorption spectra at 4.5% volume for different morphologies.

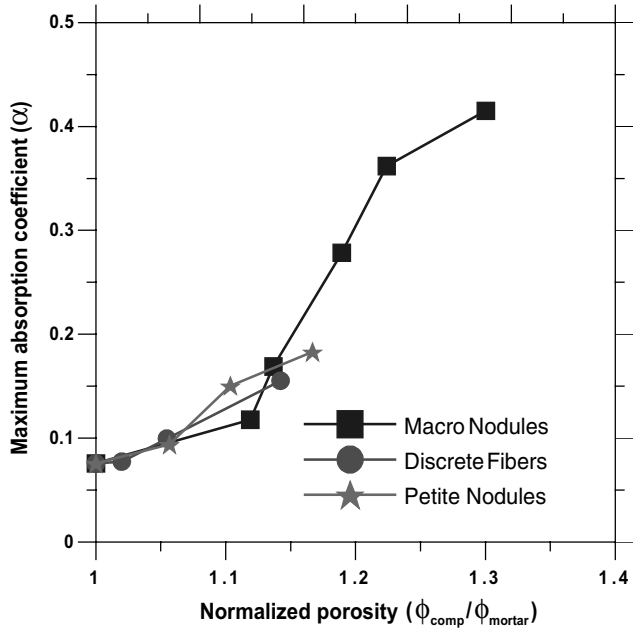

Fig. 5. Variation of maximum absorption coefficient with normalized porosity.

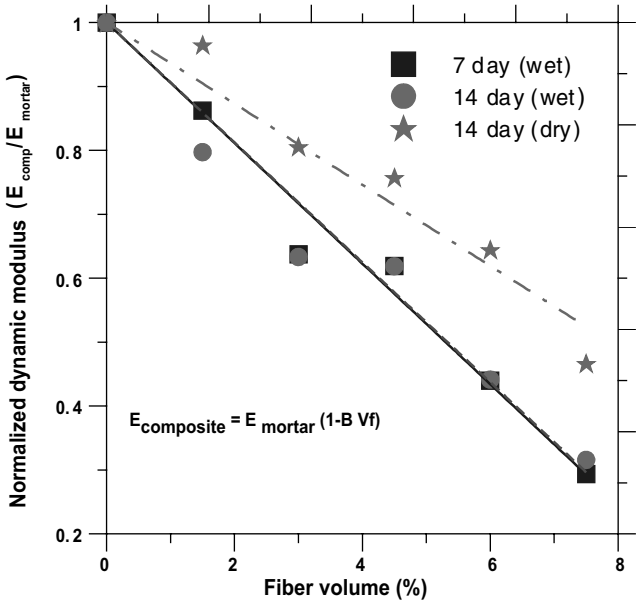

Fig. 6. Influence of fiber volume on dynamic modulus of elasticity (composites with macro-nodules).

4.2.2. Influence of porosity on absorption coefficient

Acoustic absorption is closely related to porosity [19–21]. Though it is understood that the porosity accessible to the sound waves is provided by the fiber clumps, it can be safely assumed that the total composite porosity as a function of fiber volume is some indicator of accessible porosity. The variation of maximum acoustic absorption coefficient in relation to the normalized porosity of the composites is shown in Fig. 5, which indicates an increase in maximum absorption coefficient with porosity. It can also be noted that all the three fiber types demonstrate similar response.

4.3. Dynamic modulus of elasticity

The dynamic modulus of elasticity is a function of frequency, and in composite materials, it depends on constituent properties and morphology of the individual phases [19]. The variation of normalized dynamic modulus ($E_{\text{composite}}/E_{\text{mortar}}$) with fiber volume for composites containing macro-nodules for two ages of curing and moisture condition is shown in Fig. 6. This figure depicts a gradual reduction in dynamic modulus with increase in fiber content. Moisture condition "wet" implies that the testing was done immediately after removing the specimen from 98% RH and "dry" indicates that the testing was done after conditioning the specimens at 105 °C for 24 h after the desired moist curing duration and then allowing it to return to ambient conditions.

The dynamic elastic modulus of the composite at any fiber volume can be related to that of the mortar as

$$E_{\text{composite}} = E_{\text{mortar}}(1 - BV_{\text{f}}) \tag{5}$$

The constant B is invariant for "wet" composites, irrespective of the curing duration. B for "dry" composites is found to be less than that of the wet composites, indicating that wet composites exhibit higher loss in modulus with increasing fiber volume.

A comparison of reduction in dynamic modulus of all the fibrous systems is shown in Fig. 7; the reduction in

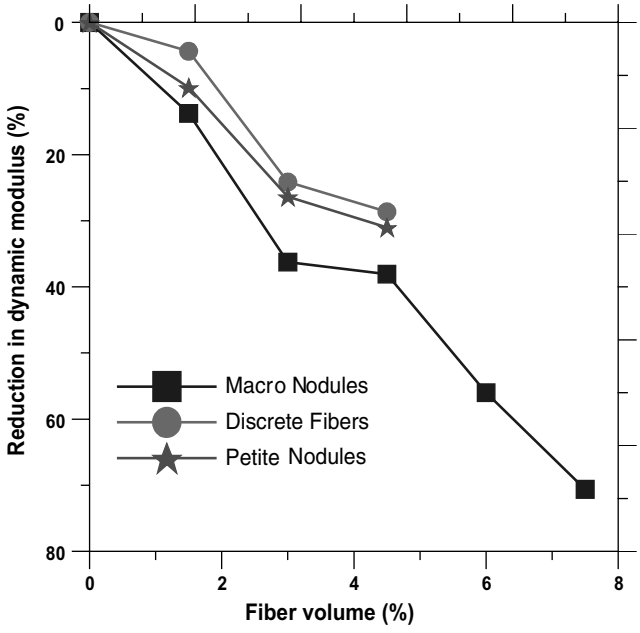

Fig. 7. Reduction in dynamic modulus of elasticity as a function of fiber volume.

modulus is highest for composites reinforced with macro-nodules, followed by those with petite nodules and then by discrete fibers. An increase in composite porosity with the addition of fibers can be attributed to this behavior—higher loss in modulus exhibited by the system with higher porosity.

4.4. Elastic damping in cellulose–cement composites

Damping defines the energy dissipation properties of a material. Viscoelastic materials can be used for damping mechanical vibrations and dissipating sound waves [22,23]. Damping in concrete is believed to be associated with the presence of water and air voids, microcracks, and acoustical impedance mismatch at the boundaries of different component phases. Damping is sensitive not only to the morphology of individual phases in a multiphase system but also to their spatial relations and individual displacements.

4.4.1. Influence of fiber volume and morphology on specific damping capacity

For specimens with macro-nodules, Fig. 8 shows the relationship between fiber content and specific damping capacity for two different ages of curing and three different moisture conditions (wet, dry, and rewetted). There is a marked increase in damping capacity with an increase in fiber content, especially for wet specimens. This may be attributed to the fact that an increase in volume of macro-nodules increases the stiffness mismatch, resulting in higher energy dissipation in the material than it would have for a sample without fibers.

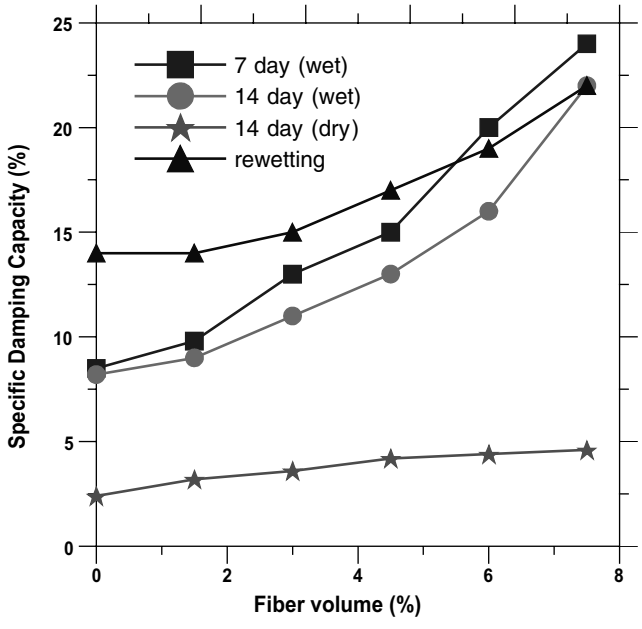

Fig. 8. Relationship between fiber volume and specific damping capacity (composites with macro-nodules).

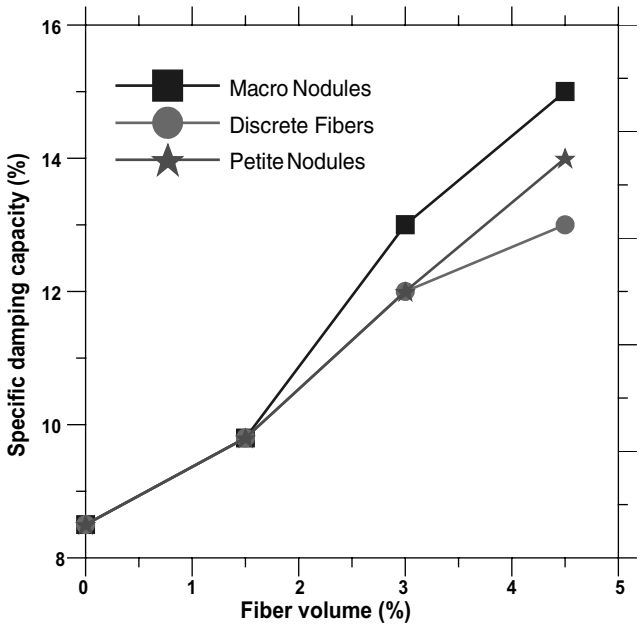

Fig. 9. Comparison of specific damping capacities of composites with different fiber types (7 day wet condition).

This is also consistent with observations from a study on damping mechanisms in hardened pastes, mortar and concrete which indicated that the damping capacity is related to the percentage of water-filled pores in the system [24], with increased moisture leading to a higher degree of damping. Higher volumes of macro-nodules effectively increase the amount of water-filled pores in the system, thereby resulting in high damping capacity values. For the same curing conditions, it can be observed that the damping capacity decreases with age, probably due to reduction in porosity and pore water content as a result of cement hydration. The reduction, though, is not very large in this case.

The specific damping capacity was found to be dependent on the fiber morphology also, as seen from Fig. 9, which shows its variation with fiber content at the age of 7 days, in the wet condition. For low fiber volumes, there is no appreciable difference in damping capacity between the three kinds of fibers investigated. Discrete fibers and petite nodules do not seem to be very different as far as damping capacities of their composites are concerned, whereas composites with macro-nodules show higher damping than the others. Macro-nodules were found to be effective in increasing the damping capacity of the composite, when added at higher fiber volumes.

4.4.2. Influence of moisture condition on specific damping capacity

The damping capacity of all specimens showed a large degree of sensitivity to moisture content. The values were reduced to one-fifth of the measured saturated

values for composites reinforced with 7.5% macro-nodules when the specimens were dried at 105 °C. The loss of moisture and development of microcracking may have opposing effects on damping [24]. The presence of microcracks increases damping whereas the loss of moisture decreases damping. When the specimens are dried at 105 °C, there are chances of formation of microcracks, but it appears that the increase in damping capacity due to microcracking is much smaller than the decrease due to water loss. As a result, dry specimens possess a smaller damping capacity than wet ones. The variation in damping capacity with fiber volume is also smaller for dried specimens. This brings out another interesting observation. Though the acoustical mismatch may seem to be the driving force for increased damping of composites with higher fiber volumes, the influence of presence of large amounts of water in these mixes cannot be neglected. It appears that both, the vibration of water molecules in the pores and the presence of porous fibers, dissipate significant amount of energy.

On rewetting of the 14 day old specimens, it can be seen that, for composites with macro-nodules, the damping capacity increases again. The increase this time is very significant and the value is higher than that observed for 7 day moist cured mixes, especially at low fiber contents. This could be due to the synergistic effects of both microcracking as well as the presence of water molecules. At higher fiber contents, this value approaches the damping capacity observed for 7 day and 14 day wet composites.

4.4.3. Stiffness–loss relationships for cellulose–cement composites

The loss tangent (the tangent of the phase angle between stress and strain in sinusoidal loading) is another useful measure of material damping characteristics. It is also defined as the ratio of the imaginary and the real parts of the complex dynamic modulus E^* ($E^* = E' + iE''$; storage modulus $E' = E\cos\delta$, and loss modulus $E'' = E\sin\delta$, so that loss tangent $\tan\delta = E''/E'$). Using the measured specific damping capacity ψ, the viscoelastic loss tangent can be obtained as $\tan\delta = \psi/2\pi$, which is proportional to the energy loss per cycle within the framework of linear viscoelasticity [25]. Most materials used in structural applications have very low loss tangents (≈0.01). In general, materials with high loss tangents tend to be more compliant, therefore these are generally not of structural interest. A stiff material with low to moderate loss tangents would be of use in structural damping of noise and vibration.

Stiffness–loss plot of $|E^*|$ or E' versus $\tan\delta$ (it is obvious that for composites with low damping, $|E^*|$ and E' values are very nearly the same) for composites with fiber volume ranging from 0% to 7.5% of macro-nodules is shown in Fig. 10. Increasing fiber volume results in reduced stiffness and increased loss tangent for the moist cured mixes. But when these parameters are plotted for the dried composites, it is seen that the increase in loss is not commensurate with the reduction in stiffness, the reason for which has been explained in the previous section. Stiffness–loss relationship seems to be dependent on the moisture condition of the specimens only and not necessarily on the curing duration as can be inferred from the similarity in curves for both 7 and 14 day cured specimens. The trend shows that the storage modulus is inversely related to the loss tangent ($E' = 0.2499\tan\delta^{-1.10}$ and $0.2388\tan\delta^{-1.10}$ for 7 and 14 day moist cured specimens tested wet, and $E' = 0.1019 \times \tan\delta^{-0.96}$ for oven dried specimens respectively). The constant that relates loss tangent and storage modulus can be thought of as an indicator of the moisture condition of the specimens.

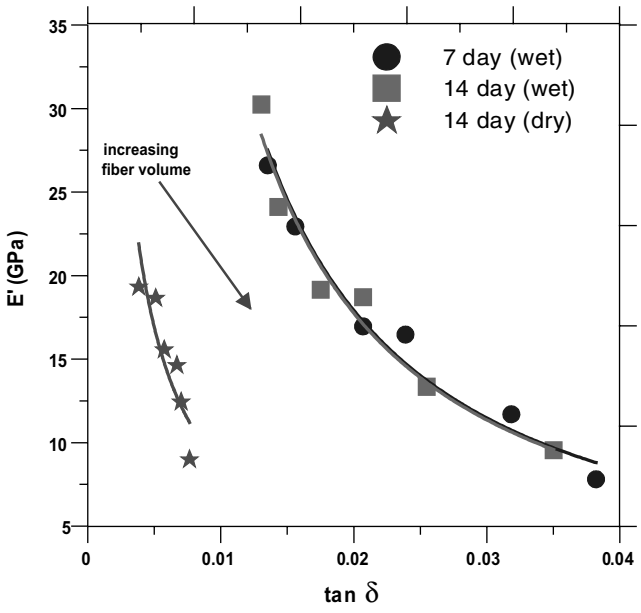

Fig. 10. Stiffness–loss map for composites with macro-nodules.

4.4.4. Influence of moisture condition on the loss tangent

A plot of fiber volume of macro-nodules versus loss tangent for saturated as well as dry composites is given in Fig. 11. It can be seen that for oven-dried composites, the increase in fiber content does not lead to a substantial increase in loss tangent as compared to saturated composites. The ratio of loss tangents in the saturated to the oven dry condition increases with increase in fiber volume. This reiterates the significance of both enhanced porosity and moisture content in increasing damping.

4.4.5. Rule of mixtures approach to stiffness–loss relationship

Since Voigt's (series) and Reuss' (parallel) rule of mixtures represent upper and lower bound for elastic constants of composites, the experimental values of

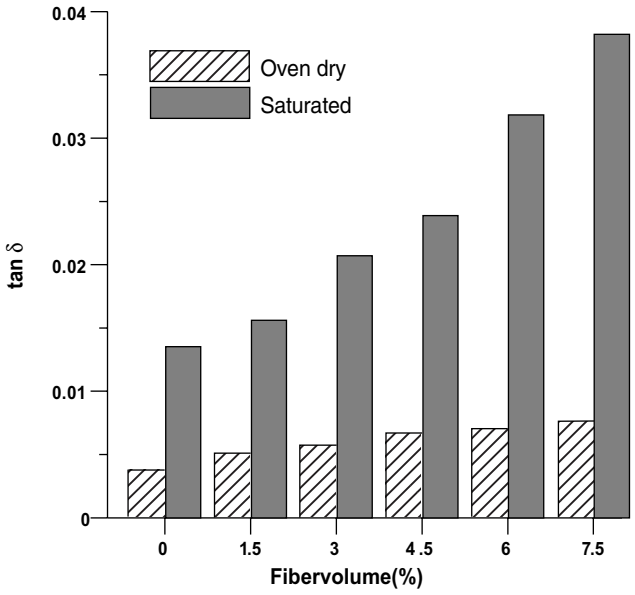

Fig. 11. Influence of moisture condition on loss tangent for different fiber volumes (composites with macro-nodules).

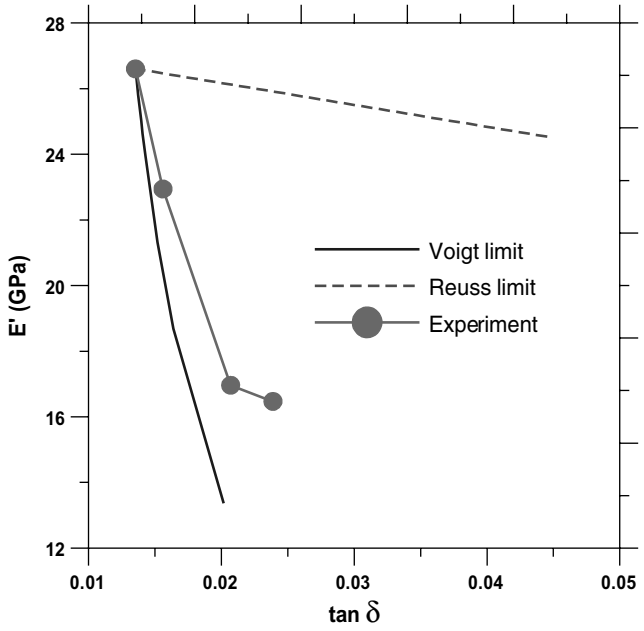

Fig. 12. Comparison of stiffness–loss relationships based on rule of mixtures with actual test data (composites with macro-nodules).

dynamic elastic modulus and loss tangent are compared with those predicted by Voigt's and Reuss' rules. The dynamic Young's moduli E can be converted into complex moduli by the relation $E^* = E e^{i\delta}$.

Considering the elastic modulus of the mortar phase as E_m and that of fiber phase as E_f and their representative volume fractions as V_m and V_f, the composite elastic modulus using Voigt's rule can be calculated as

$$E_c^* = E_m^* V_m + E_f^* V_f \tag{6}$$

and by Reuss' rule:

$$\frac{1}{E_c^*} = \frac{V_m}{E_m^*} + \frac{V_f}{E_f^*} \tag{7}$$

The loss tangents for Voigt and Reuss composites can be expressed by separating the real and imaginary parts of E_c^* [23]

$$\tan\delta_c^{\text{Voigt}} = \frac{V_m \tan\delta_m + V_f \frac{E_f'}{E_m'} \tan\delta_f}{V_m + \frac{E_f'}{E_m'} V_f} \tag{8}$$

$$\tan\delta_c^{\text{Reuss}} = \frac{(\tan\delta_m + \tan\delta_f)\left[V_m + V_f \frac{E_m'}{E_f'}\right] - (1 - \tan\delta_m \tan\delta_f)\left[V_m \tan\delta_f + V_f \tan\delta_m \frac{E_m'}{E_f'}\right]}{(1 - \tan\delta_m \tan\delta_f)\left[V_m + V_f \frac{E_m'}{E_f'}\right] + (\tan\delta_m + \tan\delta_f)\left[V_m \tan\delta_f + V_f \tan\delta_m \frac{E_m'}{E_f'}\right]} \tag{9}$$

$\tan\delta_m$ is the loss tangent for the matrix, $\tan\delta_f$ is the loss tangent for the fiber inclusion, which is assumed as 0.9 (for a soft, lossy phase), $E_m' = E_m \cos\delta_m$ and $E_f' = E_f \cos\delta_f$. E_f, based on tensile test of cellulose fibers was obtained as 2 GPa [26].

The stiffness–loss relationships for the composites with macro-nodules based on elastic moduli and loss tangents calculated using both Voigt's and Reuss' rules for 7-day moist cured composites are compared to the actual test data in Fig. 12. A small volume of fiber is seen to result in a large increase in loss for the Reuss structure whereas it results in a large reduction in stiffness with little loss for the Voigt structure. The composite with soft cellulose fiber inclusions is found to behave very similarly to the Voigt composite in that a small volume of soft material has a minimal effect on loss tangent, but reduces the stiffness to a large extent. The behavior of 14-day moist cured composites is also found to be similar.

4.4.6. Loss modulus and its prediction

The product of E' and $\tan\delta$ is the loss modulus E'', which is frequently considered as an index of damping characteristics of materials [25,27]. The loss modulus combines the storage modulus and damping capacity, thereby best reflecting the energy dissipation capability of the material.

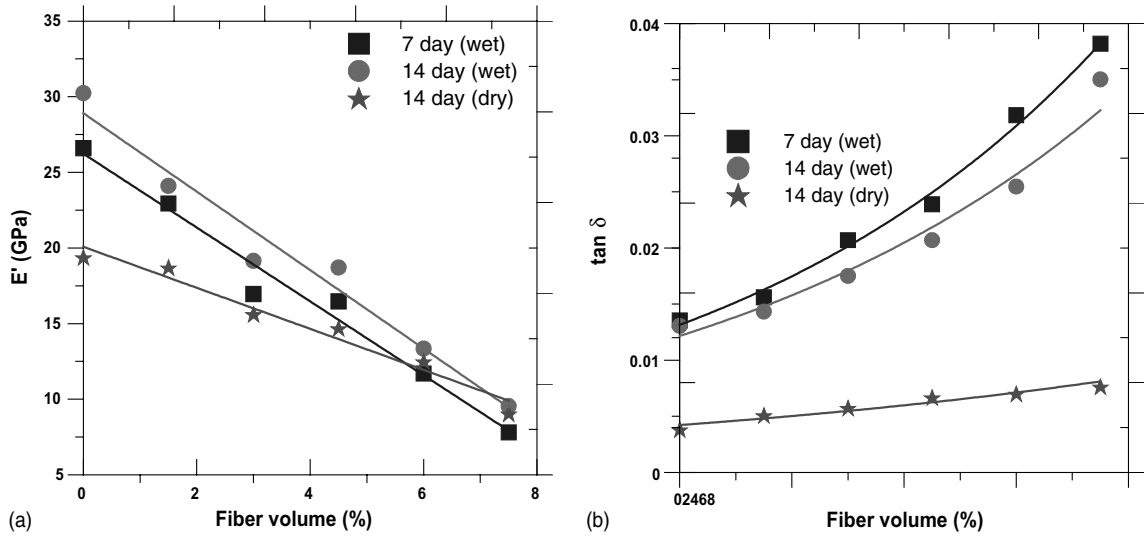

Fig. 13. Variation of (a) storage modulus and (b) loss tangent with fiber volume (composites with macro-nodules).

For a given material composition, E' and $\tan\delta$ of a composite depends on the fiber volume as well as the moisture condition of the specimen. Under a constant moisture condition, say, saturated or oven dry state, the storage modulus and loss tangent can be represented by just one parameter—the fiber volume. The plots of fiber volume against E' and $\tan\delta$ are shown in Fig. 13(a) and (b) respectively for composites with macro-nodules wet cured for 7 days, 14 days and oven dried. A fairly linear relationship can be observed between the fiber volume and storage modulus whereas the relationship between fiber volume and loss tangent can be more adequately expressed in terms of an exponential function. From the relationships between fiber volume and dynamic parameters, relationships between V_f and $E'\tan\delta$ can be easily determined. They are given as follows:

$$E'\tan\delta\ (\text{7-day}) = (0.3437 - 0.032\ V_f)e^{0.1423\,V_f} \quad (10)$$

$$E'\tan\delta\ (\text{14-day}) = (0.3527 - 0.032\ V_f)e^{0.1301\,V_f} \quad (11)$$

$$E'\tan\delta\ (\text{oven dry}) = (0.085 - 0.0057\ V_f)e^{0.0811\,V_f} \quad (12)$$

Eqs. (10) and (11) show that for saturated condition, the coefficients are similar, however they change for the oven-dried condition. These equations help to confirm the observation that the moisture condition of the specimens has a significant influence on the stiffness–loss relationship.

In Fig. 14, the loss modulus determined experimentally as well as from the equations presented above is plotted against volume of macro-nodules. The exponential predictive equations match the experimental data especially at higher fiber volumes. The deviation from curvilinear behavior in the lower ranges of fiber volume may be attributed to the fact that the loss modulus has a certain optimal value, after which a decrease in storage modulus more than compensates for an increase in loss tangent, effectively resulting in a reduced loss modulus. For the composites that are oven dried, $E'\tan\delta$ remains more or less constant with fiber volume, i.e., a decrease in storage modulus as a result of increase in fiber volume is compensated by increase in $\tan\delta$. For the other cases, as can be seen from the figure, there is an optimum fiber volume at which $E'\tan\delta$ is maximum, beyond which a decreasing storage modulus dictates the value of loss modulus. For conflicting requirements of stiffness and damping, $E'\tan\delta$ may provide a suitable parameter that can aid in the selection of materials for noise isolation and vibration damping purposes.

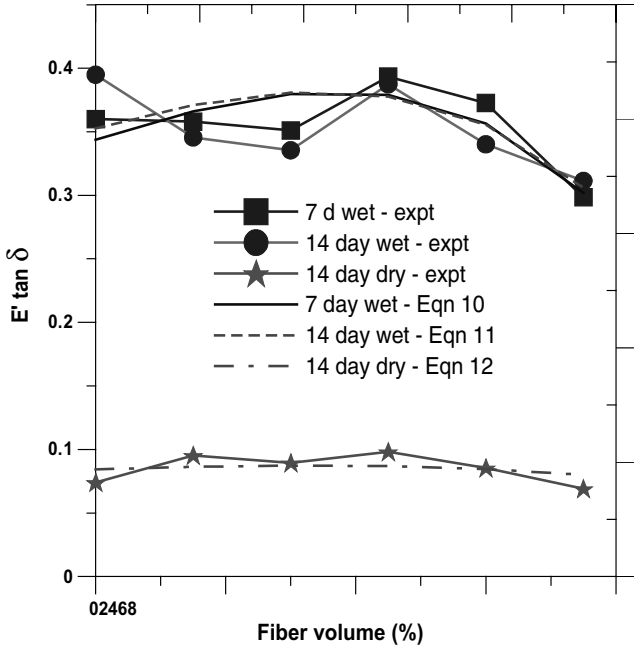

Fig. 14. Variation of loss modulus with fiber volume for different moisture conditions (composites with macro-nodules).

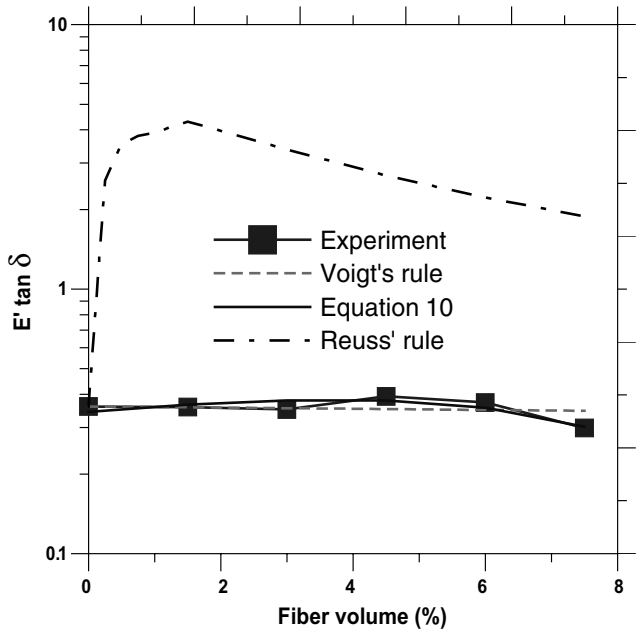

Fig. 15. Comparison of loss modulus obtained from actual test data, rules of mixtures and predictive equation (composites with macro-nodules).

The plot of $E' \tan \delta$ versus fiber volume for composites with macro-nodules cured for 7 days is also shown so as to compare the rule of mixtures with the experimental values and those obtained from Eq. (10) (Fig. 15). It can be observed that $E' \tan \delta$ values obtained from experiments and the values predicted by Voigt's rule follow the similar trend. The same could not be said of Reuss composites. This again corroborates the fact that the composite containing soft high loss inclusions in a stiff matrix, as is the case with cellulose fibers in cementitious matrix, behaves similarly to a Voigt composite. In this case also, the loss modulus predicted by Eq. (10) matches well with the experimental values.

5. Conclusions

This paper has presented the details of an experimental investigation on the acoustic absorption and damping properties of cellulose–cement composites. The morphology of the fibers and the fiber volume were substantially varied.

The following conclusions are drawn from this investigation:

1. Cellulose cement composites have the potential for absorbing sound. The absorption coefficient increases with an increase in fiber volume, possibly due to the generation of increased number of interconnected porous channels in the matrix.
2. An increase in fiber volume results in an increase in porosity for the three fiber systems investigated. Sound absorption is related to fiber morphology. Macro-nodules (large fiber clumps) are found to be more effective than discrete (small, well distributed) fibers.
3. Specific damping capacity increases with an increase in fiber content, presumably due to an increased impedance mismatch between the cementitious matrix and the cellulose phases.
4. An increase in moisture content of the specimen increases the damping capacity. Drying at 105 °C drastically reduces the damping capacity of all specimens. Though the microcracking caused by drying increases the damping, the loss of water offsets this effect to a much higher degree, resulting in reduced damping capacity.
5. The storage modulus and loss tangent for cellulose–cement composites are inversely proportional and follow an exponential relationship. For dried composites, this relation tends to be linear.
6. Cellulose cement composites containing a stiff, low-loss phase (cement matrix) and a compliant, high-loss phase (cellulose fibers) behaves similarly to a Voigt (series) composite, which shows a large reduction in stiffness and a low loss tangent.
7. A series of equations are developed to describe the loss modulus of cellulose cement composites as a function of fiber volume. These equations are found to match well with experimental values as well as those idealized to Voigt composites.
8. For water-saturated composites, there appears to be an optimal fiber volume at which $E' \tan \delta$ is maximized, beyond which a decreasing storage modulus dictates the value of loss modulus. $E' \tan \delta$ practically remains constant for oven-dried composites irrespective of fiber volume.

Acknowledgements

The authors gratefully acknowledge the support from the Institute of Safe, Quiet and Durable Highways (SQDH) and the Center for Advanced Cement Based Materials (ACBM). The assistance of Brian Wester and Julie Reimer of Weyerhaeuser in providing the cellulose fibers is gratefully appreciated. The work reported in this paper was performed in the Charles Pankow Concrete Materials Laboratory and the Herrick Labs; as such the support, which has made these labs possible, is gratefully acknowledged.

References

[1] Balaguru PN, Shah SP. Fiber reinforced cement composites. McGraw-Hill; 1992.
[2] Vinson KD, Daniel JI. Specialty cellulose fibers for cement reinforcement. In: Thin section fiber reinforced concrete and ferrocement, SP-124. Detroit: ACI; 1990. p. 1–18.

[3] Wolfe RW, Gjinolli A. Cement bonded wood composites as an engineering material. In: The use of recycled wood and paper in building applications. Madison, WI: Forest Products Society; 1996. p. 84–91.
[4] Soroushian P, Shah Z, Won JP. Optimization of wastepaper fiber–cement composites. ACI Mater J 1995;92(1):82–92.
[5] Blankenhorn PR, Silsbee MR, Blankenhorn BD, DiCola M, Kessler K. Temperature and moisture effects on selected properties of wood fiber–cement composites. Cem Concr Res 1999; 29:737–41.
[6] Soroushian P, Marikunte S. Reinforcement of cement based materials with cellulose fibers. In: Thin section fiber reinforced concrete and ferrocement, SP-124. Detroit: ACI; 1990. p. 99–124.
[7] Balaguru P. Contribution of fibers to crack reduction of cement composites during the initial and final setting period. ACI Mater J 1994;91(3):280–8.
[8] Sarigaphuti M, Shah SP, Vinson KD. Shrinkage cracking and durability characteristics of cellulose fiber reinforced concrete. ACI Mater J 1993;90(4):309–18.
[9] Soroushian P, Marikunte S, Won JP. Statistical evaluation of mechanical and physical properties of cellulose fiber reinforced cement composites. ACI Mater J 1995;92(2):172–80.
[10] Wolfe RW, Gjinolli A. Durability and strength of cement-bonded wood particle composites made from construction waste. Forest Prod J 1999;49(2):24–31.
[11] Blankenhorn PR, Blankenhorn BD, Silsbee MR, DiCola M. Effects of fiber surface treatments on mechanical properties of wood fiber–cement composites. Cem Concr Res 2001;31:1049–55.
[12] Wassilieff C. Sound absorption of wood based materials. Appl Acoust 1996;48(4):339–56.
[13] Naaman AE. SIFCON: Tailored properties for structural performance. In: Proceedings of the International RILEM/ACI Workshop 1991, High Performance Fiber Reinforced Cement Composites, Mainz, p. 18–38.
[14] Lange DA, Ouyang C, Shah SP. Behavior of cement based matrices reinforced by randomly dispersed microfibers. Adv Cem Bas Mat 1996;3:20–30.
[15] ASTM C 1437-01. Standard test method for flow of hydraulic cement mortar. ASTM International, Pennsylvania.
[16] RILEM CPC 11.3. Absorption of water by immersion under vacuum. Mater Struct 1984; 17:391–94.
[17] ASTM E 1050-98. Standard test method for impedance and absorption of acoustic materials using a tube, two microphones and a digital frequency analysis system. ASTM International, Pennsylvania.
[18] ASTM C 1259-01. Standard test method for dynamic Young's modulus, shear modulus and Poisson's ratio for advanced ceramics by impulse excitation of vibration. ASTM International, Pennsylvania.
[19] Wang CN, Torng JH. Experimental study of the absorption characteristics of some porous fibrous materials. Appl Acoust 2001;62:447–59.
[20] Marolf A, Neithalath N, Sell E, Weiss WJ, Olek J. The influence of aggregate grading on the sound absorption of enhanced porosity concrete. ACI Mater J, submitted for publication.
[21] Voronina N. An empirical model for rigid frame porous materials with high porosity. Appl Acoust 1997;51(2):181–98.
[22] Lakes RS. Extreme damping in composite materials with negative stiffness phase. Phys Rev Lett 2001;86(13):2897–900.
[23] Chen CP, Lakes RS. Analysis of high loss viscoelastic composites. J Mater Sci 1993;28:4299–304.
[24] Chowdhury SH. Damping characteristics of reinforced and partially prestressed concrete beams. PhD Thesis. Griffith University, Australia, 1999.
[25] Lakes RS, Kose S, Bahia H. Analysis of high volume fraction irregular particulate damping composites. Trans ASME 2002;124: 174–8.
[26] Kompella MK, Lambros J. Micro mechanical characterization of cellulose fibers. Polym Testing 2002;21(5):523–30.
[27] Fu X, Chung DDL. Vibration damping admixtures for cement. Cem Concr Res 1996;26(1):69–75.